JOURNAL OF THEORETICAL AND APPLIED MECHANICS
60, 3, pp. 435-448, Warsaw 2022
https://doi.org/10.15632/jtam-pl/150847

FREE VIBRATION AND BUCKLING ANALYSIS OF COMPOSITE LAMINATED SHELLS USING THE REFINED ZIGZAG THEORY

Haibo Zhang
Department of Aeronautics and Astronautics, Shenyang Aerospace University, Shenyang, China
e-mail: haibozhangcaaa@163.com

Yihang Gao
College of Aerospace Science and Engineering, National University of Defense Technology, Changsha, China, and Beijing Institute of Astronautical Systems Engineering, Beijing, China
e-mail: gaoyhddup@163.com

Dan He
Department of Aeronautics and Astronautics, Shenyang Aerospace University, Shenyang, China
Co-corresponding author Dan He, e-mail: danhe@sau.edu.cn

Wanli Yang
Department of Mechanics, Huazhong University of Science and Technology, Wuhan, China
Corresponding author Wanli Yang, e-mail: wanli_yang_nt1@163.com

In this study, a new composite laminated shell model is proposed for free vibration and stability analysis based on the refined zigzag theory (RZT). In contrast to the published shell models based on the first-order shear deformation theory (FSDT), piecewise-linear zigzag functions are utilized to provide a more realistic representation of deformation states of a transverse shear-flexible shell. In the present formulation, the governing equations and boundary conditions of composite laminated shells are established by d'Alembert's principle to obtain natural frequencies and critical buckling loadings. In order to evaluate the effectiveness and performance of the present new model for composite laminated shells, examples of free vibration and buckling analysis are carried out for cylindrical and spherical shells involving different lamination schemes and design parameters. The results are compared with the three dimensional (3D) exact, first-order and some high-order solutions in the literature. Numerical results show that the present model not only has high accuracy but also has superior computational efficiency in comparison with high-order models, such that it may show a great potential in engineering applications.

Keywords: composite, shell, buckling, free vibration, refined zigzag theory

1. Introduction

Fiber reinforced composites have high specific strength and stiffness, excellent fatigue resistance, corrosion resistance and design flexibility. In addition, shell structures have higher structural stiffness due to their curvature effect in comparison with plate structures. Therefore, shell structures made of composite materials have a wide application in engineering, such as cylindrical tanks and rocket compartments, etc. Thus, mechanical properties of these structures are extremely important to engineering, which have attracted much attention of so many scholars.

The classical plate assumes that normal to the mid-plane remains normal after deformation and does not change in length (Reddy, 2003). Although these classical assumptions are very simple, the transverse shear strains are neglected. Thus, it is only valid in thin structures. With the urgent demand for light-weight and high-strength materials in the aerospace field,

multilayered composite laminated shell structures have gradually developed into the main load-bearing structure. Owning to the above mentioned limitations, the classical shell theory (CST) is not adaptable to analysis of multilayered composite laminates with a relatively soft transverse shear modulus (Matsunaga, 2004). Therefore, transverse shear strains cannot be ignored anymore to capture the truly structural behavior. This trend urges people to try to find new modeling strategies to solve the accuracy problem of composite laminated shells. The FSDT or Reissner-Mindlin theory (Reissner, 1945; Mindlin, 1951) improves the classical laminated theory by relaxing Kirchhoff's third assumption that the transverse normal is no longer perpendicular to the middle plane after deformation. However, some researchers pointed out that it is incorrect to refer to the Reissner plate theory as a FSDT, because it would inevitably lead to displacement variation being not necessarily linear across the plate thickness (Wang *et al.*, 2001). In the following, we focus on the Mindlin FSDT in this study. It is noted that the transverse shear strain is assumed constant along the thickness direction in the Mindlin model, such that the natural surface conditions are violated. After introducing some appropriate shear correction coefficients, this theory can predict the displacement and other overall characteristics of composite laminated shells with a medium thickness. By further increasing the thickness, the calculation accuracy of this theory is obviously reduced (Iurlaro *et al.*, 2015). In order to further improve the accuracy in thick shells, scholars improved the FSDT and put forward the equivalent single-layer higher-order shear deformation theory (HSDT) (Reddy and Liu, 1985, Matsunaga, 2004). In these models, higher-order kinematic terms related to the shell thickness are added to express the in-plane displacements. Unfortunately, these models are not effective for complex cases with local load or high transverse anisotropy. The layer-wised theory (Lu and Liu, 1992; Reddy, 2003) can accurately give the global response and local response, but it contains a number of degrees of freedom proportional to the number of layers, which makes the calculation cost of thick-section laminated shells equivalent to that of 3D analysis. In addition, layer-wised theory is not easy to realize in the displacement-based finite element method. Recently, the models introducing nonlinear functions to describe the deformation of the straight line normal to the plate neutral surface have been developed to allow determination of displacements and strains (Magnucki *et al.*, 2019). They encompass both the classical "broken line" (zigzag) theory and related theories of layered structures, and may be promising in sandwich structures.

Based on the above, it is attractive to propose a model both of accuracy and efficiency for composite laminated shells from the engineering point of view. Fortunately, the zigzag theory (ZT) has the accuracy of the layer-wise theory and computational efficiency of the FSDT, in which the piecewise function in the thickness direction is added to the in-plane displacement. Therefore, the continuity of transverse shear stress is strengthened in the whole depth of composite laminated structures. The main advantage of ZT is that the unknowns no longer depend on the number of layers, which is very suitable for engineering applications. ZT has been initiated by Sciuva (1984). However, Averill and Yip (1996) pointed out two main shortcomings of Sciuva's ZT: (1) C_1 continuous functions are required to approximate the deflection in the finite element framework, because curvature is the second spatial derivative of the deflection variables. (2) The transverse shear stress calculated by the constitutive equation erroneously disappears along the fixed boundary. To solve the above problems, Tessler *et al.* (2010), Iurlaro *et al.* (2015) put forward a RZT, which has been applied to laminated beams, plates, sandwich or functionally graded structures. In this refined theory, a piecewise linear zigzag function (passing through the interface of thin plates) was added to the expression of in-plane displacement to improve the motion field of FSDT, and the lateral displacement was assumed to be constant in the whole thickness range. Therefore, the above two shortcomings of the original ZT have been overcome. In addition, the finite element is continuous in the shape function without any lateral shear force anomaly, which has a high computational efficiency and is easy to implement. Herein, it should be noted that the shear locking phenomenon may appear in the finite element

model based on the Reissner-Mindlin theory, in which the Kirchhoff constraint is enforced as the plate thickness tends to zero (Duan and Liang, 2003). This is typically too severe for the finite element model, especially if low-order polynomials are employed (Duan and Liang, 2003). Fortunately, it has been proved that the finite element models based on the RZT are simple, robust and shear locking free (Eijo *et al.*, 2013).

In view of the advantages of the RZT, a new shell model for composite laminates is proposed for vibration and buckling analysis based on the RZT. According to d'Alembert's principle, the governing equations of composite laminated cylindrical/spherical shells are derived. Then, frequencies and critical buckling loadings of composite laminated simply supported cylindrical and spherical shells are given and compared with the classical theoretical solutions, 3D elastic elasticity solutions and others in the literature. Finally, some conclusions are drawn in Section 5.

2. Displacements and strains of shells

Figure 1 schematically shows a shell with the curvature radius R_1 and R_2, wherein a, b and $2h$ are length, width and thickness of the shell, respectively. In addition, 1 and 2 are in the directions of the lines of curvature of the middle surface, and z is in the direction of the inward normal to the middle surface.

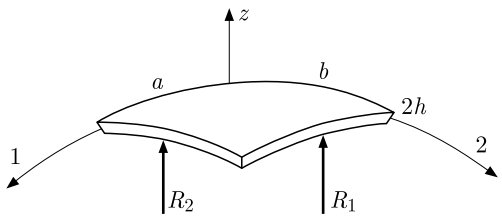

Fig. 1. Schematic diagram of a spherical shell

Based on the RZT (Iurlaro *et al.*, 2015), the displacement fields for a composite laminated shell can be expressed as (Reddy and Liu, 1985)

$$\begin{aligned} u^{(k)} &= \Big(1+\frac{z}{R_1}\Big)u(1,2,t) + z\theta_1(1,2,t) + \phi_1^{(k)}(z)\psi_1(1,2,t) \\ v^{(k)} &= \Big(1+\frac{z}{R_2}\Big)v(1,2,t) + z\theta_2(1,2,t) + \phi_2^{(k)}(z)\psi_2(1,2,t) \\ w^{(k)} &= w(1,2,t) \end{aligned} \tag{2.1}$$

where $u^{(k)}$ and $v^{(k)}$ are the in-plane displacements, $w^{(k)}$ is the deflection of any point on the shell. Correspondingly, u, v and w are the displacements on the neutral surface. t represents the time variable. The superscript k is the number of layers in laminates. The thickness in each layer is defined as $[z_{k-1} - z_k]$. In addition, θ_i $(i = 1, 2)$ are average rotation angles of the transverse normal. ϕ_i and ψ_i are piecewise linear zigzag functions and amplitude functions of RZT.

The strain fields can be obtained in an efficient way according to (Reddy and Liu, 1985)

$$\begin{aligned} &\varepsilon_{11}^{(k)} = u_{,1} + z\theta_{1,1} + \phi_1^{(k)}\psi_{1,1} + \frac{w}{R_1} \qquad \varepsilon_{22}^{(k)} = v_{,2} + z\theta_{2,2} + \phi_2^{(k)}\psi_{2,2} + \frac{w}{R_2} \\ &\gamma_{12}^{(k)} = u_{,2} + v_{,1} + z(\theta_{1,2} + \theta_{2,1}) + \phi_1^{(k)}\psi_{1,2} + \phi_2^{(k)}\psi_{2,1} \\ &\gamma_{1z} = w_{,1} + \theta_1 + \phi_{1,z}^{(k)}\psi_1 \qquad \gamma_{2z} = w_{,2} + \theta_2 + \phi_{2,z}^{(k)}\psi_2 \end{aligned} \tag{2.2}$$

where ε_{11}, ε_{22} and γ_{12} represent in-plane strains. γ_{1z} and γ_{2z} are transverse shear strains. Moreover, "," denotes the derivative with respect to the given coordinate.

The constitutive equation in the k-th layer of the shell can be shown as

$$\begin{Bmatrix}\sigma_{11}\\ \sigma_{22}\\ \tau_{12}\\ \tau_{2z}\\ \tau_{1z}\end{Bmatrix}^{(k)} = \begin{bmatrix}C_{11} & C_{12} & C_{16} & 0 & 0\\ C_{12} & C_{22} & C_{26} & 0 & 0\\ C_{16} & C_{26} & C_{66} & 0 & 0\\ 0 & 0 & 0 & Q_{22} & Q_{12}\\ 0 & 0 & 0 & Q_{12} & Q_{11}\end{bmatrix}^{(k)} \begin{Bmatrix}\varepsilon_{11}\\ \varepsilon_{22}\\ \gamma_{12}\\ \gamma_{2z}\\ \gamma_{1z}\end{Bmatrix}^{(k)} \tag{2.3}$$

In the formula, $C_{ij}^{(k)}$ $(i,j=1,2,6)$ and $Q_{\alpha\beta}^{(k)}$ $(\alpha,\beta=1,2)$ are the transformed elastic stiffness coefficients at the k-th ply referred to the (x,y,z) coordinate system (Reddy and Liu, 1985). We ignore σ_z due to the plane-stress condition (Tessler *et al.*, 2010).

Moreover, the piecewise linear zigzag functions can be written as (Tessler *et al.*, 2010), $a=1,2$

$$\begin{aligned}
&\phi_a^{(1)} = (z+h)\Big(\frac{G_a}{Q_{aa}^{(1)}}-1\Big) && k=1\\
&\phi_a^{(k)} = (z+h)\Big(\frac{G_a}{Q_{aa}^{(k)}}-1\Big) + \sum_{i=2}^{k} 2h^{(i-1)}\Big(\frac{G_a}{Q_{aa}^{(i-1)}}-\frac{G_a}{Q_{aa}^{(k)}}\Big) && k=2,\dots,N\\
&z\in[z_{(k-1)},z_{(k)}] \qquad z_{(0)}=-h \qquad z_{(k)}=z_{(k-1)}+2h^{(k)} && k=1,\dots,N
\end{aligned} \tag{2.4}$$

in which

$$[G_1,G_2]^{\mathrm{T}} = \left[\left(\frac{1}{2h}\int_{-h}^{h}\frac{dz}{Q_{11}^{(k)}}\right)^{-1},\left(\frac{1}{2h}\int_{-h}^{h}\frac{dz}{Q_{22}^{(k)}}\right)^{-1}\right]^{\mathrm{T}} \tag{2.5}$$

3. Governing equations and boundary conditions

In this Section, the governing equations and related boundary conditions for composite laminated shells are derived based on d'Alembert's principle (Iurlaro *et al.*, 2015).

The principle of virtual work can be expressed as

$$\delta U + \delta W_1 - \delta W = 0 \tag{3.1}$$

where δU, δW and δW_1 are the internal, external virtual works and the work done by the inertia force, respectively. They can be expressed as

$$\begin{aligned}
\delta U &= \int_{s_m}\int_{-h}^{h}(\sigma_{11}^{(k)}\delta\varepsilon_{11}^{(k)}+\sigma_{22}^{(k)}\delta\varepsilon_{22}^{(k)}+\tau_{12}^{(k)}\delta\gamma_{12}^{(k)}+\tau_{1z}^{(k)}\delta\gamma_{1z}^{(k)}+\tau_{2z}^{(k)}\delta\gamma_{2z}^{(k)})\,dz\,ds\\
&= \int_{s_m}\Big[N_1\delta u_{,1}+\frac{N_1}{R_1}\delta w+M_1\delta\theta_{1,1}+M_1^{\phi}\delta\psi_{1,1}+N_2\delta v_{,2}+\frac{N_2}{R_2}\delta w+M_2\delta\theta_{2,2}\\
&\quad+M_2^{\phi}\delta\psi_{2,2}+N_{12}(\delta u_{,2}+\delta v_{,1})+M_{12}(\delta\theta_{1,2}+\delta\theta_{2,1})+M_{12}^{\phi_1}\delta\psi_{1,2}+M_{12}^{\phi_2}\delta\psi_{2,1}\\
&\quad+Q_1(\delta w_{,1}+\delta\theta_1)+Q_1^{\phi}\delta\psi_1+Q_2(\delta w_{,2}+\delta\theta_2)+Q_2^{\phi}\delta\psi_2\Big]\,ds\\
\delta W &= \int_{s_m}(q\delta w)\,dS+\int_{c_\sigma}\int_{-h}^{h}(T_1\delta u_1^{(k)}+T_2\delta u_2^{(k)}+T_z\delta u_z^{(k)})\,ds\,dz\\
&= \int_{s_m}(q\delta w)\,dS+\int_{c_\sigma}\Big(\overline{N}_{1n}\delta u+\frac{\overline{M}_{1n}}{R_1}\delta u+\overline{M}_{1n}\delta\theta_1+\overline{M}_{1n}^{\phi_1}\delta\psi_1+\overline{N}_{2n}\delta v\\
&\quad+\frac{\overline{M}_{2n}}{R_2}\delta v+\overline{M}_{2n}\delta\theta_2+\overline{M}_{2n}^{\phi_2}\delta\psi_2+\overline{V}_{zn}\delta w\Big)\,d\Gamma
\end{aligned} \tag{3.2}$$

$$\delta W_1 = -\int\limits_{sm}\int\limits_{-h}^{h} \rho^{(k)}(\ddot{u}^{(k)}\delta u^{(k)} + \ddot{v}^{(k)}\delta v^{(k)} + \ddot{w}\delta w)\, dz\, ds = -\int\limits_{sm} \Big[\Big(I_0\ddot{u} + \frac{2I_1\ddot{u}}{R_1} + \frac{I_2\ddot{u}}{R_1^2} + I_1\ddot{\theta}_1 + I_2\frac{\ddot{\theta}_1}{R_1} + I_0^{\phi_1}\ddot{\psi}_1 + \frac{I_1^{\phi_1}\ddot{\psi}_1}{R_1}\Big)\delta u + \Big(I_0\ddot{v} + \frac{2I_1\ddot{v}}{R_2} + \frac{I_2\ddot{v}}{R_2^2} + I_1\ddot{\theta}_2 + \frac{I_2\ddot{\theta}_2}{R_2} + I_0^{\phi_2}\ddot{\psi}_2 + \frac{I_1^{\phi_2}\ddot{\psi}_2}{R_2}\Big)\delta v + I_0\ddot{w}\delta w + \Big(I_1\ddot{u} + \frac{I_2\ddot{u}}{R_1} + I_2\ddot{\theta}_1 + I_1^{\phi_1}\ddot{\psi}_1\Big)\delta\theta_1 + \Big(I_1\ddot{v} + \frac{I_2\ddot{v}}{R_2} + I_2\ddot{\theta}_2 + I_1^{\phi_2}\ddot{\psi}_2\Big)\delta\theta_2 + \Big(I_0^{\phi_1}\ddot{u} + \frac{I_1^{\phi_1}\ddot{u}}{R_1} + I_1^{\phi_1}\ddot{\theta}_1 + I_2^{\phi_1}\ddot{\psi}_1\Big)\delta\psi_1 + \Big(I_0^{\phi_2}\ddot{v} + \frac{I_1^{\phi_2}\ddot{v}}{R_2} + I_1^{\phi_2}\ddot{\theta}_2 + I_2^{\phi_2}\ddot{\psi}_2\Big)\delta\psi_2\Big]\, ds$$

where S_m is the neutral surface, T_1, T_2 and T_z are traction stresses prescribed on the boundary surface, and q is the external force applied to the middle surface along the z direction. The superscript $n = 1, 2$. c_σ is the circumference of a hyperbolic shell. The forces and moments are defined as

$$\begin{aligned}
\mathbf{N}_m^{\mathrm{T}} &= [N_1, N_2, N_{12}] = \int\limits_{-h}^{h} [\sigma_{11}^{(k)}, \sigma_{12}^{(k)}, \tau_{12}^{(k)}]\, dz \\
\mathbf{M}_b^{\mathrm{T}} &= [M_1, M_1^{\phi}, M_2, M_2^{\phi}, M_{12}, M_{12}^{\phi_1}, M_{12}^{\phi_2}] \\
&= \int\limits_{-h}^{h} [z\sigma_{11}^{(k)}, \phi_1^{(k)}\sigma_{11}^{(k)}, z\sigma_{22}^{(k)}, \phi_2^{(k)}\sigma_{22}^{(k)}, z\tau_{12}^{(k)}, \phi_1^{(k)}\tau_{12}^{(k)}, \phi_2^{(k)}\tau_{12}^{(k)}]\, dz \\
\mathbf{Q}_s^{\mathrm{T}} &= [Q_2, Q_2^{\phi}, Q_1, Q_1^{\phi}] = \int\limits_{-h}^{h} [\tau_{2z}^{(k)}, \beta_2^{(k)}\tau_{2z}^{(k)}, \tau_{1z}^{(k)}, \beta_1^{(k)}\tau_{1z}^{(k)}]\, dz \\
(\overline{N}_{1n}, \overline{M}_{1n}, \overline{M}_{1n}^{\phi}, \overline{N}_{2n}, \overline{M}_{2n}, \overline{M}_{2n}^{\phi}, \overline{V}_{zn}) &= \int\limits_{-h}^{h} (T_1, zT_1, \phi_1^{(k)}T_1, T_2, zT_2, \phi_2^{(k)}T_2, T_z)\, dz
\end{aligned} \tag{3.3}$$

In addition, the mass moment of inertia is defined as follows

$$\begin{aligned}
(I_0, I_1, I_2) &= \int\limits_{-h}^{h} \rho^{(k)}(1, z, z^2)\, dz \\
(I_0^{\phi_1}, I_1^{\phi_1}, I_2^{\phi_1}, I_0^{\phi_2}, I_1^{\phi_2}, I_2^{\phi_2}) &= \int\limits_{-h}^{h} \rho^{(k)}(\phi_1^{(k)}, z\phi_1^{(k)}, \phi_1^{(k)}\phi_1^{(k)}, \phi_2^{(k)}, z\phi_2^{(k)}, \phi_2^{(k)}\phi_2^{(k)})\, dz
\end{aligned} \tag{3.4}$$

where $\rho^{(k)}$ is density of the material in the k-th layer.

Substituting (3.2) into (3.1) and distributing the integral, the equilibrium equation expressed by the internal forces and moments can be obtained

$$\begin{aligned}
\delta u: &\quad N_{1,1} + N_{12,2} = I_0\ddot{u} + \frac{2I_1\ddot{u}}{R_1} + \frac{I_2\ddot{u}}{R_1^2} + I_1\ddot{\theta}_1 + \frac{I_2\ddot{\theta}_1}{R_1} + I_0^{\phi_1}\ddot{\psi}_1 + \frac{I_1^{\phi_1}\ddot{\psi}_1}{R_1} \\
\delta v: &\quad N_{12,1} + N_{2,2} = I_0\ddot{v} + \frac{2I_1\ddot{v}}{R_2} + \frac{I_2\ddot{v}}{R_2^2} + I_1\ddot{\theta}_2 + \frac{I_2\ddot{\theta}_2}{R_2} + I_0^{\phi_2}\ddot{\psi}_2 + \frac{I_1^{\phi_2}\ddot{\psi}_2}{R_2} \\
\delta w: &\quad Q_{1,1} + Q_{2,2} + q - \frac{N_1}{R_1} - \frac{N_2}{R_2} + \Lambda(w) = I_0\ddot{w} \\
\delta\theta_1: &\quad M_{1,1} + M_{12,2} - Q_1 = I_1\ddot{u} + \frac{I_2\ddot{u}}{R_1} + I_2\ddot{\theta}_1 + I_1^{\phi_1}\ddot{\psi}_1
\end{aligned} \tag{3.5}$$

$$\delta\theta_2: \quad M_{12,1}+M_{2,2}-Q_2=I_1\ddot{v}+\frac{I_2\ddot{v}}{R_2}+I_2\ddot{\theta}_2+I_1^{\phi_2}\ddot{\psi}_2$$

$$\delta\psi_1: \quad M_{1,1}^{\phi}+M_{12,2}^{\phi_1}-Q_1^{\phi}=I_0^{\phi_1}\ddot{u}+\frac{I_1^{\phi_1}\ddot{u}}{R_1}+I_1^{\phi_1}\ddot{\theta}_1+I_2^{\phi_1}\ddot{\psi}_1$$

$$\delta\psi_2: \quad M_{12,1}^{\phi_2}+M_{2,2}^{\phi}-Q_2^{\phi}=I_0^{\phi_2}\ddot{v}+\frac{I_1^{\phi_2}\ddot{v}}{R_2}+I_1^{\phi_2}\ddot{\theta}_2+I_2^{\phi_2}\ddot{\psi}_2$$

where

$$\Lambda(w)=(\Lambda_1 w_{,1}+\Lambda_{12}w_{,2})_{,1}+(\Lambda_{12}w_{,1}+\Lambda_2 w_{,2})_{,2} \tag{3.6}$$

In the above, Λ_1, Λ_2 and Λ_{12} are critical loads.

The boundary conditions are

$$\begin{aligned}
&u=\overline{u} \quad \text{or} \quad N_1n_1+N_{12}n_2=\overline{N}_{1n} && v=\overline{v} \quad \text{or} \quad N_{12}n_1+N_2n_2=\overline{N}_{2n}\\
&w=\overline{w} \quad \text{or} \quad Q_1n_1+Q_2n_2=\overline{N}_{zn} && \theta_1=\overline{\theta}_1 \quad \text{or} \quad M_1n_1+M_{12}n_2=\overline{M}_{1n}\\
&\theta_2=\overline{\theta}_2 \quad \text{or} \quad M_{12}n_1+M_2n_2=\overline{M}_{2n} && \psi_1=\overline{\psi}_1 \quad \text{or} \quad M_1^{\phi}n_1+M_{12}^{\phi_1}n_2=\overline{M}_{1n}^{\phi}\\
&\psi_2=\overline{\psi}_2 \quad \text{or} \quad M_{21}^{\phi_2}n_1+M_2^{\phi}n_2=\overline{M}_{2n}^{\phi}
\end{aligned} \tag{3.7}$$

Therefore, the constitutive relation of composite laminated shells can be rewritten in a matrix form

$$\begin{Bmatrix}\mathbf{N}_m\\ \mathbf{M}_b\\ \mathbf{Q}_s\end{Bmatrix}=\begin{bmatrix}\mathbf{A} & \mathbf{B} & \mathbf{0}\\ \mathbf{B}^{\mathrm{T}} & \mathbf{D} & \mathbf{0}\\ \mathbf{0} & \mathbf{0} & \mathbf{G}\end{bmatrix}\begin{Bmatrix}\mathbf{e}_m\\ \mathbf{e}_b\\ \mathbf{e}_s\end{Bmatrix} \tag{3.8}$$

The undefined components in (3.8) are shown in Appendix A. It is noted that the present shell model can degenerate into the following models:

1) a spherical shell when $R_1=R_2=R$,
2) a cylindrical shell when $R_1=\infty$,
3) a plate when $R_1=R_2=\infty$.

4. Numerical examples

4.1. Series solutions under a simply supported boundary condition

In this Section, series solutions are given for vibration and buckling analysis of the composite laminated shell under a simply supported boundary condition. The simply supported conditions on four sides yield that

$$v=w=\theta_2=\psi_2=0 \qquad N_1=M_1=M_1^{\theta}=0 \qquad \text{along} \qquad x\in[0,a] \tag{4.1}$$

and

$$u=w=\theta_1=\psi_1=0 \qquad N_2=M_2=M_2^{\theta}=0 \qquad \text{along} \qquad y\in[0,b] \tag{4.2}$$

Therefore, the trial function satisfying all boundary conditions can be taken as follows by omitting the terms related to the critical loads

$$\begin{aligned} w &= W \sin\frac{m\pi\xi_1}{a}\sin\frac{n\pi\xi_2}{b}\exp(\mathrm{i}\omega_{mn}t) \\ \begin{Bmatrix} u \\ \theta_1 \\ \psi_1 \end{Bmatrix} &= \begin{Bmatrix} U \\ \Theta_1 \\ \Psi_1 \end{Bmatrix} \cos\frac{m\pi\xi_1}{a}\sin\frac{n\pi\xi_2}{b}\exp(\mathrm{i}\omega_{mn}t) \\ \begin{Bmatrix} v \\ \theta_2 \\ \psi_2 \end{Bmatrix} &= \begin{Bmatrix} V \\ \Theta_2 \\ \Psi_2 \end{Bmatrix} \sin\frac{m\pi\xi_1}{a}\cos\frac{n\pi\xi_2}{b}\exp(\mathrm{i}\omega_{mn}t) \end{aligned} \tag{4.3}$$

where $U, V, W, \Theta_1, \Theta_2, \Psi_1, \Psi_2$ are unknown amplitudes of the variables, which can be determined by satisfaction of the equilibrium equations. ω_{mn} are circular frequencies. ξ_1 and ξ_2 represent coordinates of the direction 1 and 2. In addition, $\mathrm{i}^2 = -1$.

Substitute equations (4.3) into equations (3.5) to obtain the following five homogeneous algebraic equations

$$(\mathbf{K} - \omega^2\mathbf{M})[U, V, W, \theta_1, \theta_2, \psi_1, \psi_2]^{\mathrm{T}} = \mathbf{0} \tag{4.4}$$

in which $\mathbf{K}$ is the stiffness matrix and $\mathbf{M}$ is the mass matrix. ω is the natural frequency.

For a free vibration problem, solving the natural vibration frequency of laminated shells can be transformed into solving the eigenvalue problem of Eq. (4.4).

Moreover, the natural frequency disappears in a buckling problem, and the stability equation can be expressed as the following eigenvalue form in a uniaxial compression case

$$(\mathbf{K} + \Lambda_1\mathbf{G})[U, V, W, \theta_1, \theta_2, \psi_1, \psi_2]^{\mathrm{T}} = \mathbf{0} \tag{4.5}$$

where $\mathbf{G}$ is the geometric matrix caused by the initial axial stress. Λ_1 is the critical buckling load.

4.2. Free vibration of spherical and cylindrical shells

The free vibration analysis is firstly carried out in cross-ply composite laminated cylindrical shells. In order to evaluate the accuracy of the present model, the results are compared with the existing ones, i.e. 3D exact/first-order/high-order and others. It is noted that the materials and geometric parameters used in this Section are the same as those in the literature. If without another statement, the material parameters in the following are taken as

$$\begin{aligned} &\frac{E_1}{E_2} = 25 \qquad G_{12} = G_{13} = 0.5E_2 \qquad G_{23} = 0.2E_2 \\ &\nu_{12} = \nu_{13} = \nu_{23} = 0.25 \end{aligned} \tag{4.6}$$

The fundamental frequencies without the other statement are normalized as

$$\varpi = \frac{\omega a^2}{100(2h)}\sqrt{\frac{\rho}{E_2}} \tag{4.7}$$

Table 1 lists the fundamental frequencies of a $0°/90°$ composite laminated cylindrical shell in different radius-to-side and thickness-to-side ratios. It is noted that the Poisson ratios are taken as $\nu_{13} = 0.03$ and $\nu_{23} = 0.4$ in this table (Bhimaraddi, 1991). The results predicted by the present model are assessed by comparing with the 3D exact solutions and other ones based on the parabolic shear deformation theory (PSD), FSDT and CST. It is obvious that

the present results agree well with the 3D exact ones, which shows the accuracy of the present model. In addition, the difference between the PSD and present model is decreased with the increasing radius-to-side ratios. The results based on the FSDT predicts lower values in most cases, but the CST predicts higher values. Table 2 further examines the accuracy of the present model by comparing with another 3D model proposed by Ye and Soldatos (1994). Moreover, the results predicted by the high-order zigzag model and refined sinusoidal model are also listed for comparison. It is observed that Kumar's high-order zigzag model has not significantly improved the accuracy in comparison with the linear zigzag model in the present two-layer case. This phenomenon is also shown in Touratier's refined sinusoidal model, wherein the sine function may be expanded by many polynomial terms. Therefore, the efficiency of the present model is shown due to no high-order terms in the displacement fields.

Table 1. Non-dimensional fundamental frequencies of a $0^\circ/90^\circ$ composite laminated cylindrical shell in different radius-to-side and thickness-to-side ratios ($\varpi = \omega a\sqrt{\rho/E_2}$, $R_1 = \infty$, $a = b$)

R_2/a	$2h/a$	3D [2]	Present	PSD [2]	FSDT [2]	CST [2]
1	0.05	0.78683	0.783823	0.79993	0.79798	0.80580
	0.1	1.04085	1.05376	1.09819	1.07475	1.14313
	0.15	1.29099	1..32041	1.38174	1.33274	1.54124
2	0.05	0.57252	0.573939	0.58000	0.57733	0.58723
	0.1	0.93627	0.939802	0.95664	0.93653	1.01398
	0.15	1.25377	1.26069	1.28933	1.23527	1.45781
3	0.05	0.52073	0.521585	0.52516	0.52222	0.53294
	0.1	0.91442	0.916098	0.92642	0.90563	0.98505
	0.15	1.24500	1.25042	1.20563	1.21316	1.43751
4	0.05	0.50110	0.501663	0.50415	0.50109	0.51217
	0.1	0.90613	0.907888	0.91506	0.89403	0.97408
	0.15	1.24090	1.24752	1.25977	1.20454	1.42910
5	0.05	0.49167	0.492143	0.49402	0.49091	0.50216
	0.1	0.90200	0.904227	0.90953	0.88840	0.96870
	0.15	1.23849	1.24652	1.25551	1.20020	1.42464
10	0.05	0.47859	0.479236	0.47997	0.47677	0.48827
	0.1	0.89564	0.899883	0.90150	0.88026	0.96074
	0.15	1.23374	1.24628	1.24875	1.19342	1.41709
20	0.05	0.47509	0.476069	0.47625	0.47304	0.48459
	0.1	0.89341	0.899241	0.89904	0.87779	0.95819
	0.15	1.23140	1.24704	1.24626	1.19100	1.41400

[2] – Bhimaraddi (1991)

Table 2. Non-dimensional fundamental frequencies of a $0^\circ/90^\circ$ composite laminated cylindrical shell in a fixed thickness-to-side ratio ($\varpi = \omega a\sqrt{\rho/E_2}$, $a = b$, $2h/a = 0.1$, $R_1 = \infty$)

Theory R/a	1	Diff [%]	2	Diff [%]	4	Diff [%]	5	Diff [%]	10	Diff [%]	20	Diff [%]
[24]	1.06973	0	0.94951	0	0.91155	0	0.90616	0	0.89778	0	0.89477	0
Present	1.05376	1.49	0.93980	1.02	0.90789	0.40	0.90423	0.21	0.89988	−0.23	0.89924	−0.5
[8]	1.06545	0.4	0.94891	0.06	0.91368	−0.23	0.90892	−0.30	0.90180	−0.45	0.89946	−0.52
[23]	–	–	–	–	–	–	0.91060	−0.49	0.90257	−0.53	0.90011	−0.60

[24] – Ye and Soldatos (1994), [8] – Kumar *et al.* (2013), [23] – Touratier (1992)

Table 3 shows the dimensionless frequencies of the composite laminated cylindrical shell in different lamination schemes and length-to-radius ratios. It is noted that the material parameters in Table 3 are taken as

$$\frac{E_1}{E_2} = 40 \qquad E_3 = E_2 \qquad G_{12} = G_{13} = 0.6E_2$$
$$G_{23} = 0.5E_2 \qquad \nu_{12} = \nu_{13} = \nu_{23} = 0.25 \tag{4.8}$$

Table 3. Non-dimensional fundamental frequencies of a composite laminated circular cylindrical shell in different lamination schemes and length-to-radius ratios ($2h/R_2 = 0.2$, $R_1 = \infty$, $a = L$)

Theory	0°/90°				0°/90°/0°				TAEs
	$L/R_2 = 1$	Diff	$L/R_2 = 2$	Diff	$L/R_2 = 1$	Diff	$L/R_2 = 2$	Diff	
[13]	0.1012	0	0.1908	0	0.1226	0	0.2242	0	0
Present	0.1081	6.82%	0.2157	13.05%	0.1139	7.10%	0.2240	0	6.74%
[10]	0.0984	2.77%	0.1823	4.45%	0.1101	10.20%	0.1994	11.06%	7.12%
[9]	–	–	–	–	0.1014	17.29%	0.1885	15.92%	16.61%
HSDT [7]	0.0804	20.55%	0.1566	17.92%	0.1007	17.86%	0.1777	20.74%	19.27%
FSDT [7]	0.0791	21.84%	0.1552	18.66%	0.1004	18.11%	0.1779	20.65%	19.82%

[13] – Malekzadeh *et al.* (2008), [10] – Li and Wang (2016)
[9] – Lam *et al.* (2000), [7] – Khdeir *et al.* (1989)
TAEs – calculated by averaging absolute values of all particular errors

The 3D exact solutions by Malekzadeh *et al.*, (2008) are utilized as a benchmark to evaluate the accuracy of the present new model. It is noted that the state-space technique solutions of Khdeir *et al.* (1989), Ritz method results of Lam *et al.* (2000) and asymptotic solutions of Li and Wang (2016) are also listed for comparison. It is found that the accuracy of the fundamental frequencies predicted by the present model is the highest in comparison with other simplified 2D models. In addition, the results show that the TAEs of previous low/high-order models (FSDT/HSDT) are over 10%, which is three times as high as those predicted by the present model.

Tables 4 and 5 further show the dimensionless fundamental frequencies in different lamination schemes, side-to-radius ratios and side-to-thickness ratios. It is observed that there is a tiny difference among the five models, i.e. the present, FSDT, Reddy's HSDT, Mantari's new HSDT and Thakur's new HSDT in a large side-to-thickness ratio. This is because the effect of transverse shear strains is very weak in this case, and even the classical plate/shell theory has a good prediction. However, the difference becomes obvious when $a/2h = 10$. In general, it is observed that the present solutions are roughly consistent with the previous high-order models in the 0°/90° and 0°/90°/0° cases, while the model based on the FSDT under-predicts the fundamental frequencies in the 0°/90° case and over-predicts those in the 0°/90°/0° case. In addition, it is different from the results in Table 3, which shows that the first-order model agrees well with the 3D exact solutions in the 0°/90° laminate case due to the shear correction coefficient. Nevertheless, it highly depends on the material and design parameters, such as the elastic modulus and ply angle. Therefore, the shear correction coefficients are different in different cases. It is noted that the present model shows a high accuracy in the 0°/90°/0° case in comparison with the 3D exact solutions.

Moreover, the present model is very efficient with respect to those high-order models. By comparing with Mantari's new HSDT (Mantari *et al.*, 2011), the present linear zigzag terms are more convenient than the Mantari shear strain shape function $2.85^{-2(z/2h)^2} z$. It is noted that some logarithmic terms even show in the strain components in Mantari's new HSDT. By comparing with Thakur's new HSDT both of them have 7 unknowns, but z^2 and z^3 terms occur in the displacement fields in Thakur's new HSDT (Thakur *et al.*, 2017). In summary, the present

Table 4. Non-dimensional fundamental frequencies of a composite laminated cylindrical shell/plate ($\varpi = \omega a^2/(2h)\sqrt{\rho/E_2}$, $a = b$)

R_2/a $R_1 = \infty$	Theory	0°/90°		3D [3]	0°/90°/0°		3D [3]
		$a/2h = 100$	$a/2h = 10$	$a/2h = 10$	$a/2h = 100$	$a/2h = 10$	$a/2h = 10$
5	Present	16.6874	9.0423	8.7954	20.3269	11.6015	11.5007
	FSDT [11]	16.6880	8.9082	–	20.332	12.2070	–
	HSDT [11]	16.6900	9.0230	–	20.3300	11.8500	–
	[14]	16.7030	9.1254	–	20.3277	11.7469	–
	[22]	16.6846	8.9560	–	20.2959	11.7440	–
10	Present	11.8384	8.9988	8.8530	16.6126	11.5586	11.4630
	FSDT [11]	11.8310	8.8879	–	16.6250	12.1730	–
	HSDT [11]	11.8400	8.9790	–	16.6200	11.8000	–
	[14]	11.8440	9.0453	–	16.6156	11.7053	–
	[22]	11.8412	8.9474	–	16.6152	11.7501	–
20	Present	10.2683	8.9924	8.8829	15.5423	11.5478	11.4535
	FSDT [11]	10.2650	8.8900	–	15.5560	12.1660	–
	HSDT [11]	10.2700	8.9720	–	15.5500	11.7910	–
	[14]	10.2707	9.0207	–	15.5458	11.6948	–
	[22]	10.2786	8.9542	–	15.5593	11.7540	–
50	Present	9.7834	8.9935	8.9013	15.2288	11.5449	11.4508
	FSDT [11]	9.7816	8.8951	–	15.2440	12.1630	–
	HSDT [11]	9.7830	8.9730	–	15.2400	11.7900	–
	[14]	–	–	–	–	–	–
	[22]	9.7969	8.9618	–	15.2507	11.7566	–
100	Present	9.7122	8.9947	8.9075	15.1835	11.5445	11.4504
	FSDT [11]	9.7180	8.8974	–	15.1980	12.1630	–
	HSDT [11]	9.7120	8.9750	–	15.1900	11.7900	–
	[14]	9.7127	9.0085	–	15.1872	11.6915	–
	[22]	9.7264	8.9649	–	15.2061	11.7575	–
Plate	Present	9.6885	8.9964	8.9131	15.1683	11.5443	11.2503
	FSDT [11]	9.6873	8.8998	–	15.1830	12.1620	–
	HSDT [11]	9.6880	8.9760	–	15.1700	11.7900	–
	[14]	9.6886	9.0065	–	15.1721	11.6913	–
	[22]	9.7031	8.9684	–	15.1913	11.7584	–

[3] – Chern and Chao (2000), [11] – Lu and Liu (1992)
[14] – Mantari *et al.* (2011), [22] – Thakur *et al.* (2017)

model not only has a high accuracy, but also has a high efficiency to deduce the finite element method for analyzing large-scale laminated structures in the future.

4.3. Axial compression buckling of a circular cylindrical shell

In this Section, we pay attention to the buckling analysis of composite laminated circular cylindrical shells under the uniaxial compression. The difference between the results predicted by the present model and the models based on the FSDT/HSDT are shown in Fig. 2 in different thickness-to-radius ratios. The material constants are taken as (30).

Figure 2 shows the trend of critical buckling loads. In the thickness-to-radius ratio, the radius is constant. It can be seen that the results predicted by the present model are consistent with the results based on the FSDT and Reddy's HSDT, when the radius-to-thickness ratio is small.

Table 5. Free vibration of a composite laminated spherical shell/plate

R/a	Theory	$0°/90°$		[3]	$0°/90°/0°$		[3]
		$a/2h = 100$	$a/2h = 10$	$a/2h = 10$	$a/2h = 100$	$a/2h = 10$	$a/2h = 10$
5	Present	28.8392	9.3543	9.2008	31.0142	11.7925	11.6713
	FSDT [11]	28.8250	9.2309	–	30.9930	12.3720	–
	HSDT [11]	28.8400	9.3370	–	31.0200	12.0600	–
	[14]	28.8391	9.3654	–	31.0161	11.9593	–
	[22]	28.8019	9.2676	–	30.9669	11.9484	–
10	Present	16.7121	9.0874	8.9870	20.3463	11.6017	11.5140
	FSDT [11]	16.7060	8.9841	–	20.3470	12.2150	–
	HSDT [11]	16.7100	9.0860	–	20.3500	11.8600	–
	[14]	16.7121	9.0980	–	20.3492	11.7592	–
	[22]	16.7031	9.0408	–	20.3415	11.8009	–
20	Present	11.8442	9.0191	8.9322	16.6164	11.5559	11.4702
	FSDT [11]	11.8410	8.9212	–	16.6270	12.1760	–
	HSDT [11]	11.8400	8.9990	–	16.6200	11.8100	–
	[14]	11.8442	9.0295	–	16.6201	11.7084	–
	[22]	11.8499	8.9846	–	16.6306	11.7662	–
50	Present	10.0647	8.9999	8.9168	15.4058	11.5448	11.4554
	FSDT [11]	10.0630	8.9034	–	15.4240	12.1650	–
	HSDT [11]	10.0600	8.9800	–	15.4200	11.7900	–
	[14]	–	–	–	–	–	–
	[22]	10.0774	8.9700	–	15.4305	11.7583	–
100	Present	9.7839	9.9972	8.9145	15.2289	11.5439	11.4523
	FSDT [11]	9.7826	8.9009	–	15.2440	12.1630	–
	HSDT [11]	9.7840	8.9770	–	15.2400	11.7900	–
	[14]	9.7840	9.0074	–	15.2327	11.6920	–
	[22]	9.7980	8.9684	–	15.2514	11.7578	–
Plate	Present	9.6885	8.9964	8.9138	15.1682	11.5443	11.4503
	FSDT [11]	9.6873	8.8998	–	15.1830	12.1620	–
	HSDT [11]	9.6880	8.9760	–	15.1700	11.7900	–
	[14]	9.6886	9.0065	–	15.1721	11.6913	–
	[22]	9.7031	8.9684	–	15.1913	11.7584	–

[3] – Chern and Chao (2000), [11] – Lu and Liu (1992)
[14] – Mantari *et al.* (2011), [22] – Thakur *et al.* (2017)

However, obvious differences appear with the increasing thickness-to-radius ratios. For example, the first-order model is relatively deviated from the high-order model when $2h/R = 0.3$. This is because the FSDT assumes that the in-plane displacement changes linearly along the thickness, which artificially increases the stiffness of the structure. While Reddy's high-order model uses a third-order function to describe the in-plane displacement, such that it is generally closer to the actual situation than the first-order model. Between the above two models, the present model is based on kinematics of the FSDT and adds an in-plane linear zigzag function along the thickness direction, such that the shear correction coefficients are not needed any more. It is noted that the differences between the present model and the models based on the FSDT and HSDT are about 5% when $2h/R = 0.3$.

Table 6 further lists the non-dimensional critical buckling loads in different laminates and shell theories. It is observed that the CST over-predicts the critical buckling load. In addition, the results are consistent with the high-order model and the first-order model with the shear correction coefficient.

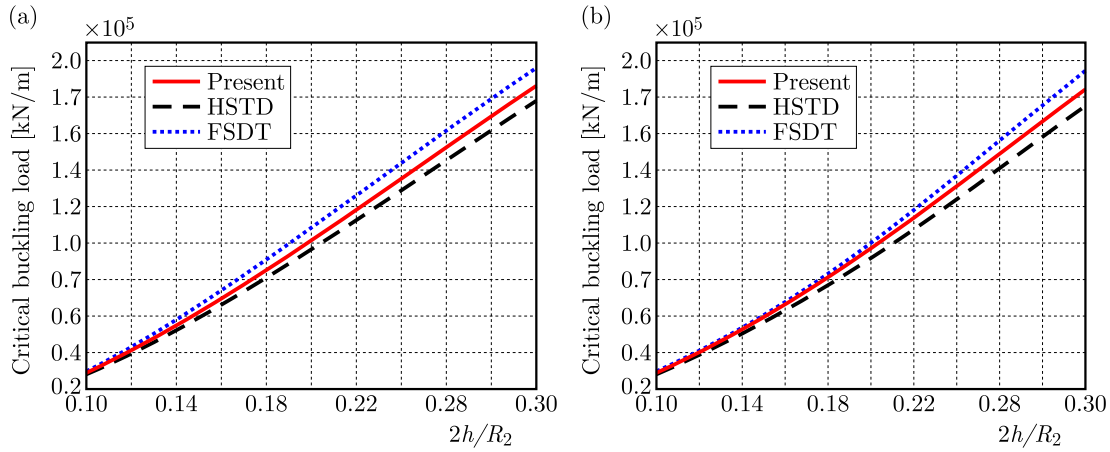

Fig. 2. Variation of critical buckling loads with different thickness-radius ratios: (a) 0°/90°/0°, (b) 0°/90°/0°/90°

Table 6. Non-dimensional critical buckling loads in different laminates and shell theories ($\overline{\Lambda} = \Lambda L^2/(100(2h)^3 E_2)$, $L/R_2 = 1$, $R_2/2h = 10$)

Lamination	Theory	Critical buckling loads
0°/90°	Present	0.1662
	HSDT (Khdeir *et al.*, 1989)	0.1687
	FSDT (Khdeir *et al.*, 1989)	0.1670
	CST (Khdeir, *et al.*, 1989)	0.1817
0°/90°/0°	Present	0.2858
	HSDT (Khdeir *et al.*, 1989)	0.2794
	FSDT (Khdeir *et al.*, 1989)	0.2813
	CST (Khdeir *et al.*, 1989)	0.4186
0°/90°/0°/ . . . /10 layers	Present	0.2758
	HSDT (Khdeir *et al.*, 1989)	0.2896
	FSDT (Khdeir *et al.*, 1989)	0.2898
	CST (Khdeir *et al.*, 1989)	0.3395

5. Conclusions

In this paper, the RZT is extended to free vibration and buckling problems of composite laminated cylindrical/spherical shells. Based on d'Alembert's principle, the linear eigenvalue problems of free vibration and buckling of composite laminated cylindrical/spherical shells are solved. After studying in detail the effect of lamination schemes and design parameters on the dynamic and stable performance, some observations can be drawn as follows:

- For free vibration problems, the results show that the present model can accurately predict the dynamic response of composite laminated shells. The predicted natural frequencies are more consistent with the 3D exact solutions.
- For buckling problems, obvious differences among the present model and models based on the FSDT/HSDT appear with the increasing thickness-to-radius ratios.
- The modulus ratio and lamination schemes have a great effect on the accuracy of the simplified shell theories.
- The predictive ability of the RZT on composite laminated shells has been rigorously evaluated, which proves its superior efficiency, accuracy and wide applicability.

A. Appendix

According to Tessler *et al.* (2010), the components in (3.5) are listed as follows

$$\mathbf{C}=\begin{bmatrix} C_{11} & C_{12} & C_{16} \\ C_{12} & C_{22} & C_{26} \\ C_{16} & C_{26} & C_{66} \end{bmatrix}^{(k)} \qquad \mathbf{B}_{\varphi}=\begin{bmatrix} z & \varphi_1^{(k)} & 0 & 0 & 0 & 0 & 0 \\ 0 & 0 & z & \varphi_2^{(k)} & 0 & 0 & 0 \\ 0 & 0 & 0 & 0 & z & \varphi_1^{(k)} & \varphi_2^{(k)} \end{bmatrix} \tag{A.1}$$

$$\mathbf{Q}=\begin{bmatrix} Q_{22} & Q_{12} \\ Q_{12} & Q_{11} \end{bmatrix}^{(k)} \qquad \mathbf{B}_{\beta}=\begin{bmatrix} 1 & \beta_2^{(k)} & 0 & 0 \\ 0 & 0 & 1 & \beta_1^{(k)} \end{bmatrix} \tag{A.2}$$

$$\begin{aligned} &\mathbf{A}_{3\times 3}=\int_{-h}^{h}\mathbf{C}\,dz \qquad \mathbf{B}_{3\times 7}=\int_{-h}^{h}\mathbf{C}\mathbf{B}_{\phi}\,dz \\ &\mathbf{D}_{7\times 7}=\int_{-h}^{h}\mathbf{B}_{\phi}^{\mathrm{T}}\mathbf{C}\mathbf{B}_{\phi}\,dz \qquad \mathbf{G}=\int_{-h}^{h}\mathbf{B}_{\beta}^{\mathrm{T}}\mathbf{Q}\mathbf{B}_{\beta}\,dz \end{aligned} \tag{A.3}$$

$$\begin{aligned} &\mathbf{e}_m^{\mathrm{T}}=\Big[u_{,1}+\frac{w}{R_1},v_{,2}+\frac{w}{R_2},u_{,2}+v_{,1}\Big] \\ &\mathbf{e}_b^{\mathrm{T}}=[\theta_{1,1},\psi_{1,1},\theta_{2,2},\psi_{2,2},\theta_{1,2}+\theta_{2,1},\psi_{1,2},\psi_{2,1}] \qquad \mathbf{e}_s^{\mathrm{T}}=[w_{,2}+\theta_2,\psi_2,w_{,1}+\theta_1,\psi_1] \end{aligned} \tag{A.4}$$

References

1. Averill R.C., Yip Y.C., 1996, Development of simple, robust finite elements based on refined theories for thick laminated beams, *Computers and Structures*, **59**, 529-546
2. Bhimaraddi A., 1991, Free vibration analysis of doubly curved shallow shells on rectangular planform using three-dimensional elasticity theory, *International Journal of Solids and Structures*, **27**, 897-913
3. Chern Y., Chao C.C., 2000, Comparison of natural frequencies of laminates by 3-D theory, Part II: Curved panels, *Journal of Sound and Vibration*, **230**, 1009-1030
4. Duan H.Y., Liang G.P., 2003, Mixed and nonconforming finite element approximations of Reissner-Mindlin plates, *Computer Methods in Applied Mechanics and Engineering*, **192**, 5265-5281
5. Eijo A., Oñate E., Oller S., 2013, A four-noded quadrilateral element for composite laminated plates/shells using the refined zigzag theory, *International Journal for Numerical Methods in Engineering*, **95**, 631-660
6. Iurlaro L., Gherlone M.D., Di Sciuva M., Tessler A., 2015, Refined zigzag theory for laminated composite and sandwich plates derived from Reissner's mixed variational theorem, *Composite Structures*, **133**, 809-817
7. Khdeir A.A., Reddy J.N., Frederick D., 1989, A study of bending, vibration and buckling of cross-ply circular cylindrical shells with various shell theories, *International Journal of Engineering Science*, **27**, 1337-1351
8. Kumar A., Chakrabarti A., Bhargava P., 2013, Vibration of laminated composites and sandwich shells based on higher order zigzag theory, *Engineering Structures*, **56**, 880-888
9. Lam K.Y., Ng T.Y., Qian W., 2000, Vibration analysis of thick laminated composite cylindrical shells, *AIAA Journal*, **38**, 1102-1107

10. Li Z.M., Wang M., 2016, Large-amplitude vibration analysis of 3D braided composite cylindrical shells in an elastic medium, *Journal of Aerospace Engineering*, **29**, 04015029

11. Lu X., Liu D., 1992, An interlaminar shear stress continuity theory for both thin and thick composite laminates, *Journal of Applied Mechanics*, **59**, 502-509

12. Magnucki K., Witkowski D., Magnucka-Blandzi E., 2019, Buckling and free vibrations of rectangular plates with symmetrically varying mechanical properties – Analytical and FEM studies, *Composite Structures*, **220**, 355-361

13. Malekzadeh P., Farid M., Zahedinejad P., 2008. A three-dimensional layerwise-differential quadrature free vibration analysis of laminated cylindrical shells, *International Journal of Pressure Vessels and Piping*, **85**, 450-458

14. Mantari J.L., Oktem A.S., Guedes Soares C., 2011, Static and dynamic analysis of laminated composite and sandwich plates and shells by using a new higher-order shear deformation theory, *Composite Structures*, **94**, 37-49

15. Matsunaga H., 2004, A comparison between 2-D single-layer and 3-D layerwise theories for computing interlaminar stresses of laminated composite and sandwich plates subjected to thermal loadings, *Composite Structures*, **64**, 161-177

16. Mindlin R.D., 1951. Influence of rotatory inertia and shear on flexural motions of isotropic, elastic plates, *Journal of Applied Mechanics*, **18**, 31-38

17. Reddy J.N., 2003, *Mechanics of Laminated Composite Plates and Shells: Theory and Analysis*, CRC Press

18. Reddy J.N., Liu C.F., 1985, A higher-order shear deformation theory of laminated elastic shells, *International Journal of Engineering Science*, **23**, 319-330

19. Reissner E., 1945, The effect of transverse shear deformation on the bending of elastic plates, *Journal of Applied Mechanics*, **12**, 69-76

20. Sciuva M.D., 1984, A refined transverse shear deformation theory for multilayered anisotropic plates, *Atti Accademia Science Torino*, **118**, 79-95

21. Tessler A., Di Sciuva M., Gherlone M., 2010, A consistent refinement of first-order shear deformation theory for laminated composite and sandwich plates using improved zigzag kinematics, *Journal of Mechanics of Materials and Structures*, **5**, 341-367

22. Thakur S.N., Ray C., Chakraborty S., 2017, A new efficient higher-order shear deformation theory for a doubly curved laminated composite shell, *Acta Mechanica*, **228**, 69-87

23. Touratier M., 1992, A refined theory of laminated shallow shells, *International Journal of Solids and Structures*, **29**, 1401-1415

24. Ye J., Soldatos K.P., 1994, Three-dimensional vibration of laminated cylinders and cylindrical panels with symmetric or antisymmetric cross-ply lay-up, *Composites Engineering*, **4**, 429-444

25. Wang C.M., Lim G.T., Reddy J.N., Lee K.H., 2001, Relationships between bending solutions of Reissner and Mindlin plate theories, *Engineering Structures*, **23**, 838-849

Manuscript received May 20, 2022; accepted for print May 25, 2022